International Research Journal of Engineering and Technology (IRJET) e-ISSN: 2395-0056
Volume: 07 Issue: 03 | Mar 2020 www.irjet.net p-ISSN: 2395-0072

Comparative Study on the Structural and Optical Characterization of ZnS and ZnO Nanoparticle

P.K. Upadhyay[1], Vikas Kumar Jain[2], A. K. Shrivastav[3], Ravi Sharma[4*]

[1]*Department of Physics, Govt.Nagrik Kalyan Mahavidyalaya Ahiwara, Durg (C.G.) India*
[2]*Department of Chemistry, Govt. Engineering College, Sejbahar, Raipur (C.G.) India*
[3]*Department of Physics, Dr C. V. Raman University, Kargi road kota , Bilaspur (C.G.) India*
[4]*Department of Physics, Govt. Arts and Commerce Girls College Raipur (C.G.) India*

Abstract :- *The present paper reports the synthesis and characterization of pure luminescent zinc oxide and zinc sulphide nanoparticles. Nanoparticles of zinc sulphide were prepared by chemical precipitation method using the solution of zinc chloride, sodium sulphide, mercaptoethanol (ME) was used as the capping agent, whereas, nanoparticles of zinc oxide were prepared by using the solution of zinc acetate, ammonia and thiourea was used as the capping agent. The particle sizes of nanoparticles were calculated experimentally using XRD and SEM. The particle sizes measured by XRD pattern was found to be in the range 2nm-7nm for ZnS nanoparticles and 50nm to 60nm for ZnO nanoparticles. SEM images showed agglomeration of nanoparticles. The blue-shift in absorption spectra was observed with reducing size of the nanoparticles. The FTIR spectra inferred that the stabilizing agent passivated the surface of the particles. The PL spectra of these particles were also studied. The results of the as-prepared ZnO and ZnS nanoparticles are compared with each other and also with those reported in the literature.*

Keywords: **Structural properties; photoluminescence; optical absorption spectra; ZnS, ZnO Nanoparticles.**

Introduction

Materials in the nanometer scale may exhibit physical properties, distinctively different from that of bulk [1]. Quantum confinement effect plays an important role for the particles synthesized in the nanoscale. At this scale, increase in the energy gap as well as splitting of the conduction and valence band into discrete energy levels becomes evident. The II-VI semiconductor ZnO and ZnS are used in many applications primarily due to their luminescent properties. ZnO and ZnS are commercially important II–VI semiconductors having a wide optical band gap, rendering it to be a very attractive material for optical application especially in nanocrystalline form. ZnS is a direct band gap material having band gap energy 3.67eV and a small exciton Bohr radius of ~ 4 nm, whereas, ZnO has the band gap ~ 3.37 eV, bohr exciton radius is approximately 2.34 nm and exciton-binding energy of 60 meV. Thus, ZnO is a promising candidate for the high efficient ultraviolet (UV) laser device. Owing to its wide band gap, ZnS is used in cathode ray tube, the field emission display, and the scintillator as one of the most frequently used phosphors [2 – 4]. The luminescence of ZnS has been studied by many workers [5-12]. ZnO has found numerous applications, such as biosensors, biological labels, solar cells, electrochemical cells, ultraviolet photodiodes, electrical and optical devices [13 - 19].

Synthesis of nanomaterials with the desired quality and properties is one of the key issues in nanoscience. Synthesis techniques change the optical, electrical and magnetic properties of nanomaterials. ZnO nanoparticles are prepared by several methods such as hydrothermal method, sol-gel method and simple precipitation method [20 - 22]. Optical and luminescent properties of nano ZnS prepared in the forms of thin film, powder and colloid using different synthesis techniques such as sputtering, co-evaporation, wet chemical, sol-gel, solid state, micro-wave irradiation, ultrasonic irradiation were studied in detail [23 - 33]. Different synthesis routes have also been developed and reported for preparation of nano ZnO such as thermal evaporation, pyrolysis, wet-chemical, pulsed laser deposition, chemical combustion process, electrochemical synthesis and sol-gel method [33-42].

The chemical route synthesis is used to prepare ZnS and ZnO nanoparticles. Their structural characterization by XRD, SEM, and optical characterization by UV-VIS spectrometry, FTIR and photoluminescence studies are reported in the present work. Effect of concentration of the capping agent on the particle size, structural and the luminescent properties of the ZnS and ZnO nanoparticles were investigated. The study was aimed to compare the size dependent optical and the structural properties of synthesized ZnS and ZnO nanoparticles.

Experimental

For the synthesis of nano ZnS chemical deposition technique was used [43]. In this method aqueous solution of $ZnCl_2$, mercaptoethanol (C_2H_5OSH) and Na_2S, of each solution was used for the reaction. Firstly, mercaptoethanol in a reaction vessel was added to the $ZnCl_2$ solution drop wise,while stirring it continuously. Then Na_2S was added drop wise to the same reaction vessel. The rate of mixing of solution was 1 ml per minute. The end product was then washed thoroughly in double distilled water to remove any excess of Na_2S. Finally, the solution was centrifuged at 3500 rpm and the precipitate obtained was air dried and the white colour final product was used for characterization.

Zinc acetate (Zn $(CH_3COO)_2$. $2H_2O$), thiourea ($(NH_2)_2CS$) and ammonia (25% NH_3) was used as the starting materials, for the preparation of the ZnO nano-powders. The nano ZnO powder was be prepared by dissolving zinc acetate, thiourea and ammonia in deionised water, separately. The chemical bath technique was used: 60 mL of a Zinc acetate, thiourea and ammonia solutions were mixed at ratio of 1:1:1 and rapidly heated to 80□C while continuously stirring. The prepared ZnO nanoparticles was washed with acetone, ethanol and deionized water. All the reagents of AR-grade were used without further purification.

The morphologies and sizes of as prepared ZnS and ZnO nanoparticles were determined by X-ray diffraction using Cu Kα radiation (λ = 1.5418 Å). Rigaku Rotating Anode (H-3R) diffractometer was used for X-ray diffraction patterns. XRD data were collected over the range 20□- 70□at room temperature. For scanning electron microscope (SEM), JSM – 5,600 LV was used. The particle size was calculated using the Debye-Scherrer formula. Absorption spectra of the samples prepared was recorded with the help of Perkin Elmer Model Lamda 950 UV-VIS spectrophotometer. The FTIR spectra were recorded by the help of FTIR spectrometer (SHIMADZU) in the range of 500 cm^{-1} to 4,000 cm^{-1}. For PL measurements Perkin Elmer spectroflurophotometer Model LS 45 was used.

Results and Discussions

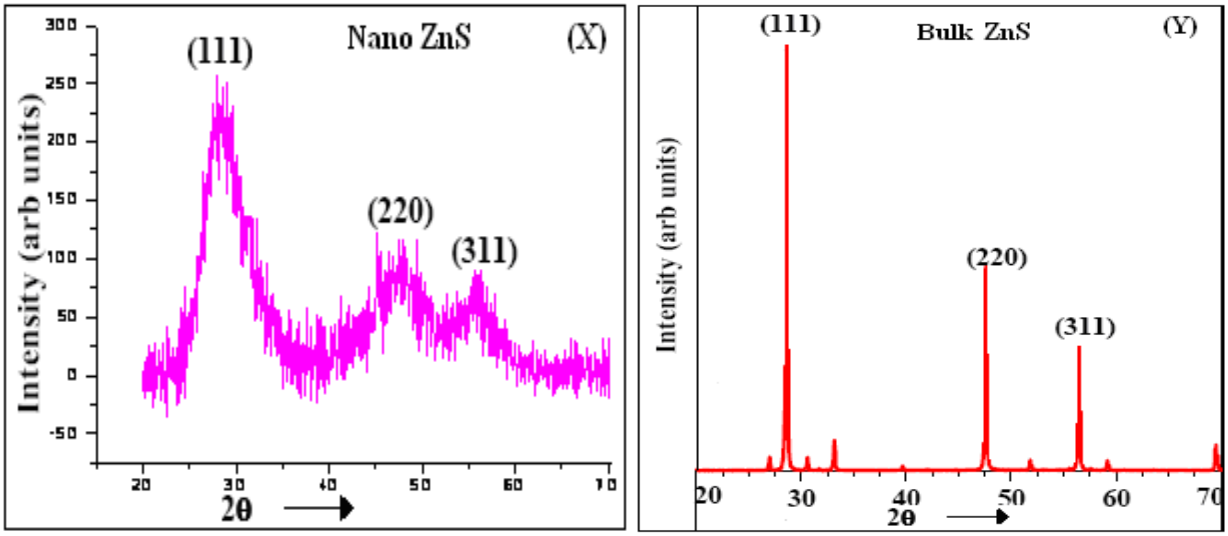

Fig.1 XRD spectra of synthesized nano ZnS and ZnS bulk

Figure 1 (Y) shows the XRD pattern of bulk crystals of ZnS and figure (X) shows the XRD patterns of the synthesized nano ZnS. Broadening in the XRD peaks could be very clearly seen from the above figures. The broadening of the peak is due to the smaller particle size large number of crystal planes. This broadening in turn causes a loss of intensity in the signal of their diffraction patterns. The sharp, narrow and high-intense peaks of the bulk particles show that it is highly crystalline and the particles are in the bigger size. The three diffraction peaks positions corresponds to the lattice planes of (1 1 1), (2 2 0) and (3 1 1) matching the zinc blende (sphalerite) ZnS crystal structure (JCPDS 5-566). The lattice parameter has been computed as 5.33 □, which is very close to the standard value (5.42 □). The size of the synthesized nano ZnS sample was 5nm.

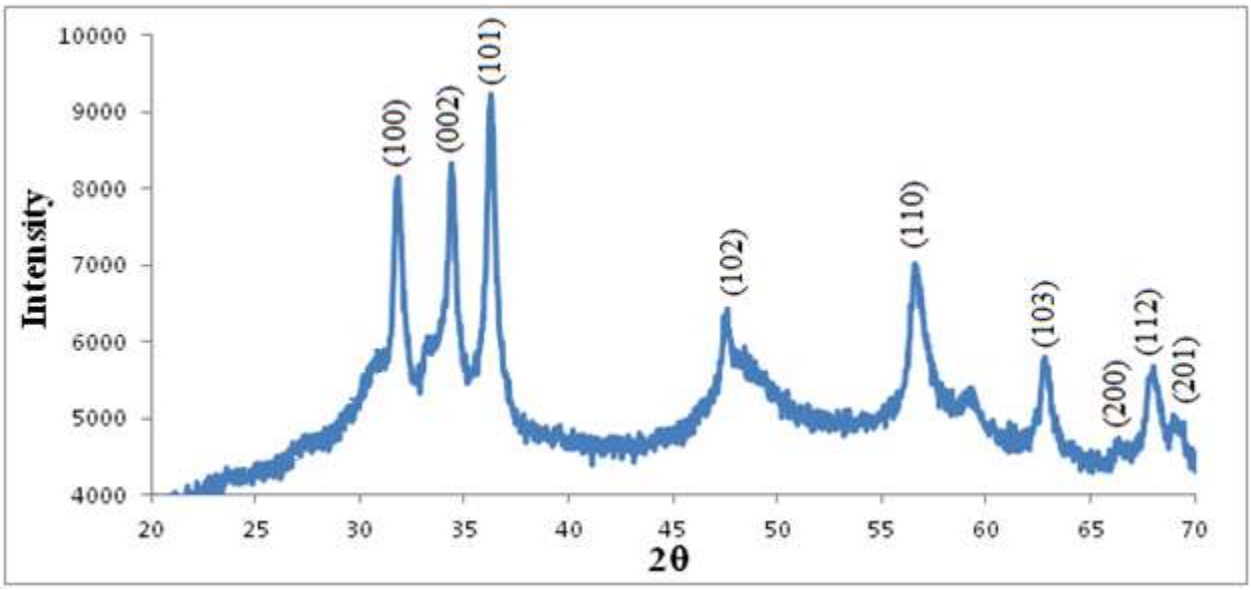

Fig.2 XRD spectra of synthesized ZnO nanoparticles

Figure 2 shows the XRD pattern of the synthesized ZnO nanoparticles. From the above figure it could be inferred that the synthesized ZnO nanoparticles are in pure phase, i.e. no impurities are seen in the XRD pattern. The peaks obtained at $2\theta^{o}$ values of 31.62, 34.33, 36.12, 47.33, 56.31, 62.64, 66.03, 67.64, and 68.73 can be attributed to the planes (100), (002), (101), (102), (110), (103), (200) and (112), (201) respectively, with hexagonal crystal structure having cell parameter a = 3.264 Å and c = 5.219 Å (JCPDS file No. 79-0208). Broadening in the XRD peaks could be seen very clearly, which confirms the nanocrystalline nature of zinc oxide. More broadening in the diffraction peaks was observed for the samples with higher concentration of the thiourea (not shown here). For all the samples the size of the particles were calculated from the first peak only. For all the samples the average crystallite size was determined from the XRD pattern parameters using Debye Scherrer equation $D = k\lambda/\beta\cos\theta$, where D is the average crystallite size, k is Scherrer's constant equal to 0.90, β is the full-width at half-maximum (FWHM), and θ is the Bragg's angle. The size of the synthesized ZnO sample was 55nm.

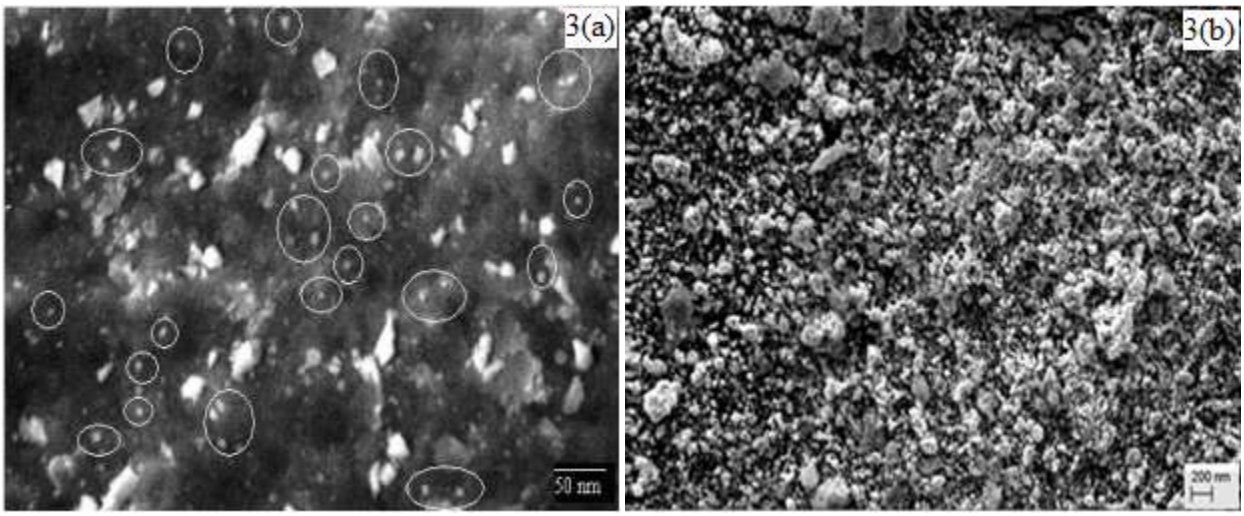

Fig. 3 SEM photograph of ZnS and ZnO nanoparticles

The SEM photograph of ZnS and ZnO nanocrystals is shown in Figure 3(a) and 3(b) respectively. From figure 3(a) it can be seen that some of the particles are agglomerated, this is due to the formation of ZnS nanoparticles during first few minute of the experiment and later these particles agglomerates and their size becomes larger. Non spherical particles are clearly visible

in the SEM photograph. The average particle sizes obtained from SEM images were in the range of 5nm to 10nm. Some of the particles are even less than 5 nm (encircled) [43]. In the figure 3(b), highly agglomeration of particles is clearly seen. Many of the particles are in the range less than 30nm. The average size of these synthesized non spherical powder ZnO nanoparticles is ~ 50 nm.

The UV–visible absorption spectra of ZnS and ZnO nanoparticles as a function of wavelength are shown in Figure 4(a) and 4(b) respectively. In both the cases, i.e., the absorption band of the ZnS nanoparticles and absorption spectra of ZnO nanoparticles shows a blue shift due to the quantum confinement effect of the excitations present in the samples as compared with the bulk. This optical phenomenon indicates that these nanoparticles have a quantum size effect [44]. Figure 4(a) shows that the optical absorption spectra of the nano ZnS measured between 400 nm-200 nm. It was found that the spectra are featureless and no absorption occurs in the visible region. The absorption peak for the synthesize nano Zns was recorded at 294nm which is much less than peak of bulk ZnS at 345nm. The peak of the samples with higher concentration of the capping agent showed a shift towards the lesser value of wave length. The optical absorption edge also showed gradual blue shift for the samples with higher concentration of the capping agent (not shown here). The characteristic absorption edge reflects the band gap of the material. In case of nano ZnO the spectra is shown between 210nm – 300nm because no absorption occurred in other region. In figure 4(b) the excitonic absorption peak of ZnO nanoparticle was found at 219 nm, which lies much below the band gap wavelength of 388 nm of bulk ZnO [45]. The peak at ~219 nm is due to inter band transition of electrons from the more inner shell to the uppermost shell. It is possible that, due to aggregation and agglomeration, particle size increases and material settled down at the bottom of container causing decrease in the absorbance [46]. This type of behavior is typical for many semiconductors due to internal electric fields within the crystal and inelastic scattering of charge carriers by phonons [47- 49].

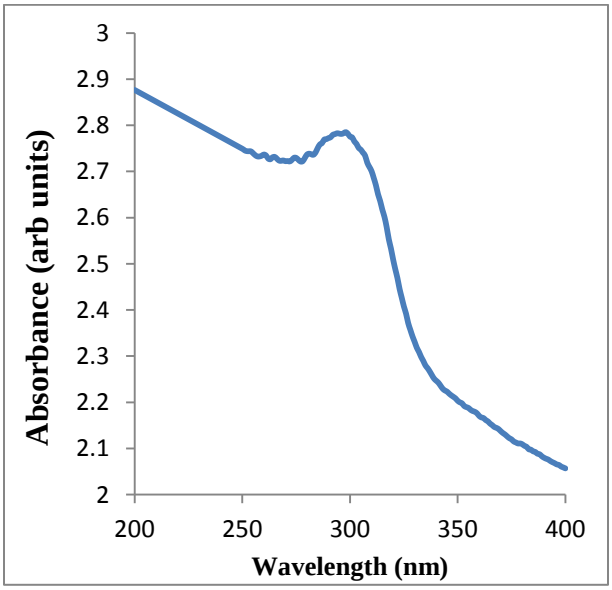

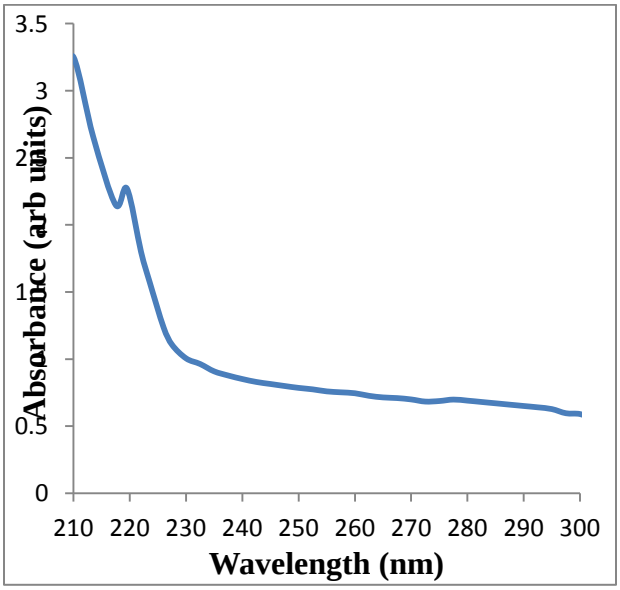

Fig. 4(a) absorption spectra of nano ZnS Fig. 4(b) absorption spectra of nano ZnO

Absorption coefficient (α) associated with the strong absorption region for both the samples of nano ZnS and nano ZnO were calculated from absorbent (A) and the sample thickness (t) using relation **α = 2.303A/t.** The optical band gap of ZnS and ZnO nanoparticles is calculated using the Tauc relation: **(αhν)$^{1/n}$ = A(hν − E$_g$)**, Where, *α* is the absorption coefficient, *hν* is the energy of incident photons and exponents *n* whose value depends upon the type the transition which may have values 1/2, 2, 3/2 and 3 corresponding to the allowed direct, allowed indirect, forbidden direct and forbidden indirect transitions, respectively. For the samples of ZnS and ZnO the value of n is 1/2.

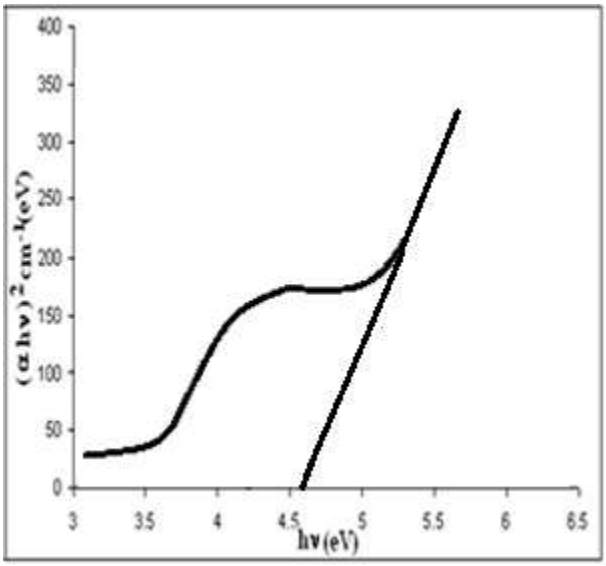

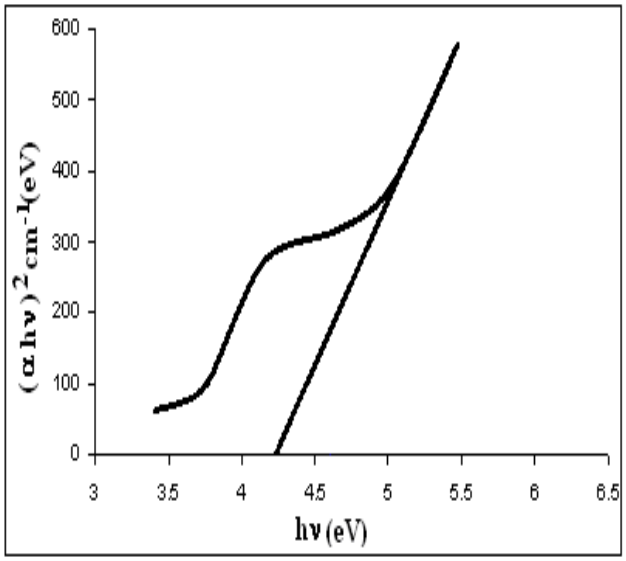

Fig. 5(a) Tau's plot of ZnS nanoparticles **Fig. 5(b) Tau's plot of ZnO nanoparticles**

Figure 5(a) shows the tau's plot of ZnS nanoparticles. The band gap calculated from the above data was 4.63eV. There is a shift of 0.93eV in the band gap as compared to the bulk ZnS (3.66eV). This is an indication that the capping agent played an important role in controlling the particle size. Figure 5(b) show the tau's plot for ZnO nanoparticles. The band gap for ZnO nanoparticles is calculated to be 4.23 eV, which is higher than reported value 3.54 eV. The increase in the band gap of the ZnO nanoparticles with the decrease in particle size may be due to a quantum confinement effect. Similar results were reported by Harish Kumar et al [50].

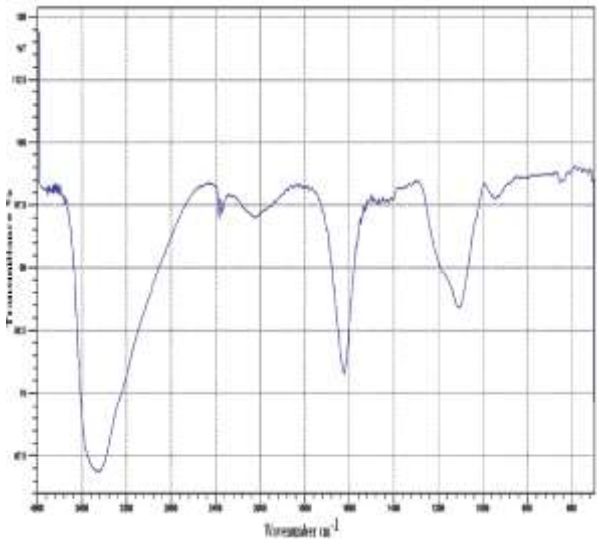

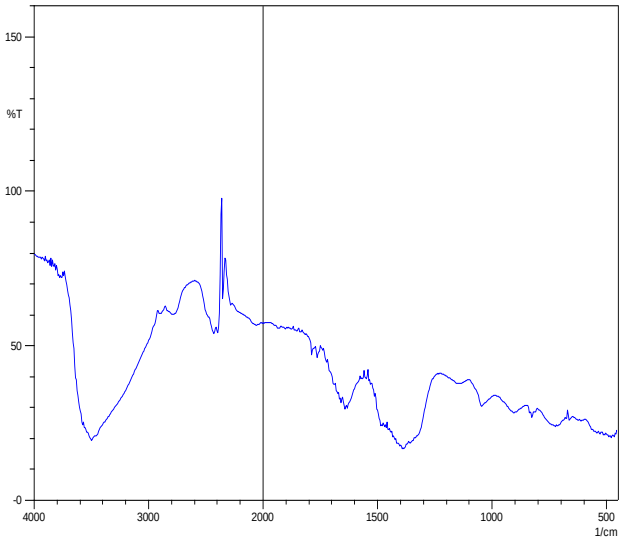

Fig. 6(a) FTIR spectra of ZnS nanoparticles **Fig. 6(b) FTIR spectra of ZnO nanoparticles**

FTIR is an effective method to reveal the composition of products. It gives the information about organic composition of the samples and the presence of various bonds in the sample. Figure 6(a) and 6(b) shows the FTIR spectra of the ZnS and ZnO nanopaticles respectively. These figures show a smooth curve. In figure 6(a) the peak at 671 cm^{-1} is assigned to the ZnS band (i.e., corresponding to sulphides). Bands around 1200 cm^{-1} and 1100 cm^{-1} are due to the characteristic frequency of inorganic ions. A comparative strong peak was observed at 1086 cm^{-1}, which is because of C- O stretching of the capping agent. The broad peak in the higher energy region at 3439 cm^{-1} is due to OH stretching and the peak at 1625 cm^{-1} is due to OH bending of adsorbed moisture in the sample and all the other peaks are attributed to the characteristic of the material. Figure 6(b) is a

typical FTIR spectrum of pure ZnO nanoparticls. The spectra show characteristic peaks at 511, 591, 671, 712, 826, 921, 1,058, 1,146, 1,386, 1,460, 1,638, 1,787, 2,448, 2,801, 3,450 cm^{-1} and some other associated peaks. The bands around 501 and 640 cm^{-1} are assigned to the Zn-O band. A strong intensity band at 1,058 cm^{-1} may be due to S-O-C stretching. The stretching vibrations assigned to the C-S linkage occur in the region of 800–600 cm^{-1} and the weak S-S stretching vibration falls between 600 - 400 cm^{-1}. The peak at 1600-1700cm^{-1}may be due to nitrogen–oxygen interaction. The distinct peaks at 1386 cm^{-1} and 1146 $cm^{-1}$are due to phosphorus–oxygen interaction, establishing the presence of covalently bonded phosphates on ZnO nanoparticles. The broad absorption peak at 3450 cm-1 can be attributed to the characteristic absorption of hydroxyl group.

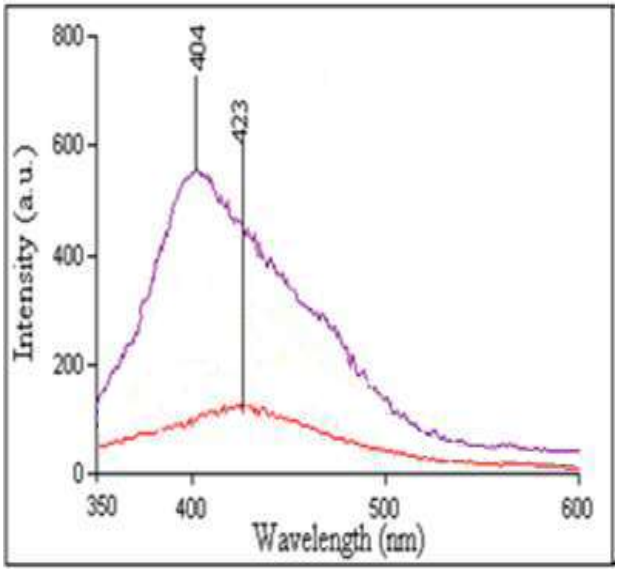

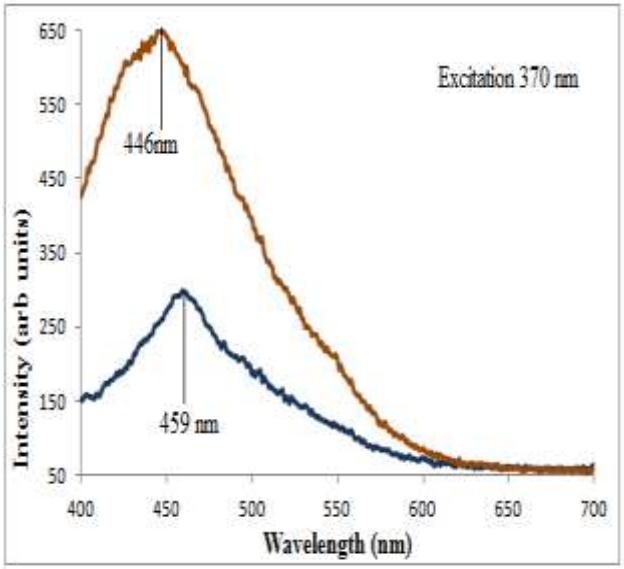

Fig. 7(a) PL of ZnS nanoparticle **Fig. 7(b) PL of ZnO Nanoparticles**

Study of the photoluminescence (PL), property of any material is interesting because it can provide valuable information on the purity and quality of the material. Luminescence studies provide information regarding defect states. In nanocrystals, the PL study reveals the information about the shift in the defect states or increase in density. Figure 7(a) and figure 7(b) shows the PL spectrum of the ZnS and ZnO nanoparticles. In figure 7 (a) the PL spectra of ZnS samples in the range 350 nm-600 nm prepared with different concentration of capping agent (10mM & 60mM). The samples were excited at 289nm. It was found that a peak at 423nm was found for the ZnS nanoparticles. The violet emission at 423 nm is due to the interstitial zinc. The peak intensity at 423 nm associated with band gap emission of ZnS was observed very less in the case of Bulk ZnS. The emission peak shows shift towards shorter wavelength with the increasing concentration of the capping agent. Stoke-shifted PL peak was obtained at 423 nm and 404 nm for 10mM and 60mM concentration of mercaptoethanol, respectively. Fig. 7(b) shows the room temperature PL spectra of the ZnO nanoparticles recorded in the range 400 nm-700 nm prepared with different concentration of thiourea. The PL measurements were recorded at excitation wavelength of 370nm. Only one peak at ~450nm is found for the ZnO nanoparticles. With increasing concentration of thiourea, stoke-shifted PL peak was obtained at 446 nm and 459 nm. It is visible that the PL emission becomes intensive and shifts towards smaller wavelength as the size of the particles is decreased. As compared to ZnS nanoparticles this emission peak shift is less towards smaller wavelength due to small change in the particle size. This PL spectra is may be because of the electron–hole recombination at a deep level emission in the band gap caused by intrinsic point defects and surface defects, e.g., oxygen vacancies, zinc interstitials, and the incorporation of hydroxyl groups in the crystal lattice during solution growth [51]. The broad band luminescence for both ZnS and ZnO nanoparticles is related to transitions from donor states to deep acceptor states.

Conclusions

The nanoparticals ZnS and ZnO have been successfully synthesized by a simple chemical reaction using aqueous medium, in which mercaptoethanol and thiourea was used as the capping agent respectively. The XRD pattern indicated the growth of the nanoparticles. SEM images show the agglomeration of nanocrystals and therefore larger size was observed whereas XRD give the extent to which regular arrangement of atoms exists and hence gives the average crystal size. XRD analysis shows that the ZnS nanoparticles are in cubical phase, whereas, the ZnO nanoparticles are in hexagonal phase. The particle size calculated

from XRD analysis for nano ZnS was found to be in the range 2nm -7nm and for nano ZnO was in the range 50-60nm. The optical absorption spectra showed blue-shift for both the samples. The blue-shift in optical absorption spectra can be explained by solid-state theory based on the delocalized electron and hole within the confined volume. The band gap calculated from the above data was 4.63eV for ZnS nanoparticle and the band gap for ZnO nanoparticles was found to be 4.23 eV. The shift in band gap for nano ZnS (0.93eV) is more prominent than for nano ZnO (0.69eV) as compared to the bulk ZnS and bulk ZnO, due to smaller size. The increase in the band gap of the ZnS and ZnO nanoparticles with the decrease in particle size is due to a quantum confinement effect. Prominent IR peaks were analyzed and assigned. The FTIR spectra inferred that the stabilizing agent passivated the surface of the particles. Nano ZnS showed more blue-shift in the peak position of photoluminescence spectra as compared to nano Zno. So, it be concluded that as per our experiment, the nano ZnS is more luminescent than nano ZnO.

References

[1] Cao G., Nanostructures and Nanomaterials: Imperial College Press, London, (2004).

[2] Okuda H., Dakada J., Iwasaki Y., Hashimoto N., Nagao C., IEEE Trans. Consumer Electron., 36 (1990), 436-439.

[3] Ghrayeb J., Jackson T.W., Daniels R., Hopper D.G.,Proc. SPIE, 3057 (1997) 237-40.

[4] Barton J.C., Ranby P.W., J. Phys. E, 10, (1997) 437-438.

[5] Kumbhojkar N., Nikesh V. V., Kshirsagar A., Mahamuni S., J. Appl. Phys.; 88 (2000), 6260 -64,.

[6] Karar N., Singh F., Mehta B.R., J. Appl. Phys., 95 (2004), 656-60.

[7] Nanda J., Sarma D.D., J. Appl. Phys., 90 (2001), 2504-10.

[8] Bol A.A., and Meijerink A., J. Phys. Chem B., 105 (2001) 10203-9, .

[9] Bhargava R.N., Gallaghar D., Hong X., Nurmikko A., Phys. Rev. Lett., 72 (1994), 416-9.

[10] Que W., Zhou Y., Lam Y.L., Chan Y.C., Kam C.H., Liu B. et. al, Appl. Phys. Lett., 73, (1998), 2727- 29

[11] Borse P.H., Deshmukh N., Shinde R.F., Date S.K., Kulkarni S.K., J. Mat. Sc.,34 (1999), 6087-6093

[12] Strukov D.B., Snider G.S., Stewart D.R., Williams R.S., Nature, 453 (2008), 80-83.

[13] X.Cao,W.Ning,D.Lil,L.Guo,SensorsActuators.B:Chem.129 (2008)268.

[14] M.BruchezJr.,M.Moronne,P.Gin,S.Weiss,A.P.Alivisatos,Science 281 (1998) 2013- 18.

[15] Z.S.Wang,C.H.Huang,Y.Y.Huang,Y.J.Hou,P.H.Xie,B.W.Zhang,H.M.Cheng, Chem. Mater.13(2001), 678- 683.

[16] H.Weller,Adv.Mater.5(1993), 88- 92.

[17] I.S.Jeong,J.H.Kim,S.Im,Appl.Phys.Lett.83(2003), 2946- 2953 .

[18] C.Feldmann,Adv.Fundam.Mater.13(2003), 101-105.

[19] J.Wang,L.Gao,Inorg.Chem.Commun.6(2003), 877- 884.

[20] P. M. Aneesh, K. A. Vanaja and M. K. Jayaraj, Proceedings of SPIE, 6639 (2007), 66390J-1.

[21] T. V. Kolekar, H. M. Yadav, S. S. Bandgar and P. Y. Deshmukh, Indian streams of research journal, 1 (2011), 1-10.

[22] S. Sivakumar, P. Venkateswarlu, V. R. Rao and N. Rao, Synthesis, International Nano letters, 3 (2013), 1- 5.

[23] Mandal S.K., Chaudhuri S., Pal A.K., Thin Solid Films, 30 (1999) 209-13.

[24] Thielsch R., B□me T., B□tcher H., Phys. Status Solidi A, 155 (1996)., 157-170,

[25] Chen W., Wang Z., Lin Z., Lin L., J. Appl. Phys., 82 (1997), 3111-15.

[26] Scholtz S.M., Vacassy R., Dutta J., Hoffmann H., J. Appl. Phys., 83 (1998), 7860-66.

[27] R. Sharma, S.J. Dhoble, D.P. Bisen, N. Brahme, B.P. Chandra, Int. J. Nanoparticles
4 (1) (2011) 64 - 76.

[28] Tan M., Cai W., Zhang L., Appl. Phys. Lett., 71, (1997), 3697- 3708,

[29] Bhattacharjee B., Ganguli D., Chaudhuri S., Pal A.K., Mater. Chem. Phys., 78 (2003), 372-379.

[30] Lu H.-Y., Chu S.-Y., Tan S.-S., J. Cryst. Growth, 269 (2004), 385-391.

[31] Zhao Y., Hong J.-M., Zhu J.-J., J. Cryst. Growth, 270 (2004), 438-445.

[32] Ni Y., Yin G., Hong J. Xu, Z., Mater. Res. Bull., 39 (2004), 1967-1972.

[33] Xu J.F., Ji W., Lin J.Y., Tang S.H., Du Y.W., Appl. Phys., A 66 (1998), 639-641.

[34] J. R. Duclère, B. Doggett, M. O. Henry, E. McGlynn, R. T. Rajendra Kumar, J.-P. Mosnier, A. Perrin and M. Guilloux-Viry, Journal of Applied Physics, 101 (2007), 3509-3517.

[35] S. Sivakumar, P. Venkateswarlu, V. R. Rao and N. Rao, International Nano letters, 3(2013), 1- 5.

[36] R. Pérez -Casero, A. Gutiérrez -Llorente, O. Pons-Y-Moll, W. Seiler, R. M. Defourneau, D. Defourneau, E. Millon, J. Perrière, P. Goldner and B. Viana, Journal of Applied Physics, 97, (2005), 54905.

[37] X. M. Teng, H. T. Fan, S. S. Pan, C. Ye and G. H. Li, Journal of Applied Physics, 100, (2006), 53507.

[38] J. S. John, J. L. Coffer, Y. Chen and R. F. Pinizzotto, Applied Physics Letter, 77 (2000), 1635.

[39] J. L. Bubendorff, J. Ebothe, A. El Hichou, R. Dounia and M. Addou, Journal of Applied Physics, 100 (2006) 14505.

[40] M. Alaoui Lamrani, M. Addou, Z. Soofiani, B. Sahraoui, J. Ebothé, A. El Hichou, N. Fellahi, J. C. Bernède and R. Dounia, Opti cs Com- munications, 277,1 (2007), 196-201.

[41] Z. Sofiani, S. Bouchta and M. Addou, Journal of Applied Physics, 101 (2007), 63104.

[42] N. Mais, J. P. Reithmaier, A. Forchel, M. Kohls, L. Spanhel and G. Müller , Applied Physics Letter, 75 (2005),1999.

[43] Ravi Sharma, International Multidisciplinary Research Journal, 1(9) (2011), 08-11,

[44] Huang, M.H.; Mao, S.; Feick, H.; Yan, H.; Wu, Y.; Kind, H.; Weber, E.; Russo, R.; Yang, P.D, Science, 292 (2001), 1897–1899.

[45] Pathik Kumbhakar, Devendra Singh, Chandra S. Tiwary, Amya K. Mitra, Chalcogenide letters 5 (2008) 387-394.

[46] T. S. Moss, G. J. Burrell, B. Ellis, Semiconductor Opto-Electronics, Butterworth & Co. Ltd. 1973.

[47] H. M. Honsi, S. A. Fayek, S. M. Al-Sayed, M. Roushdy, M. A. Soliman, Vacuum 81 (2006) 54-58.

[48] A. Sawby, M. S. Selim, S. Y. Marzouk, M. A. Mostafa, A. Hosny, Physica B: Physics of Condensed Matter 405 (2010) 3412-3420.

[49] J. P. Yang,, F. C. Meldrum, J. H. Fendler, Journal of Physical Chemistry 99 (1995), 5500-5504.

[50] Harish Kumar, Renu Rani, International Letters of Chemistry, Physics and Astronomy 14 (2013) 26-36

[51] S. Xu, Z. Wang, Nano Research 4 (2011) 1013.